Monte Carlo based water/medium stopping-power ratios for various ICRP and ICRU tissues

José M Fernández-Varea[1]**, Pablo Carrasco**[2]**, Vanessa Panettieri**[3]
and Lorenzo Brualla[4]

[1] Facultat de Física (ECM), Universitat de Barcelona, Diagonal 647, E-08028 Barcelona, Spain
[2] Servei de Radiofísica i Radioprotecció, Hospital de la Santa Creu i Sant Pau,
Sant Antoni Maria Claret 167, E-08025 Barcelona, Spain
[3] Institut de Tècniques Energètiques, Universitat Politècnica de Catalunya, Diagonal 647,
E-08028 Barcelona, Spain
[4] Physics Department, College of Science, Sultan Qaboos University, PO Box 36,
Code 123 Al-Khoud, Sultanate of Oman

E-mail: jose@ecm.ub.es

Abstract
Water/medium stopping-power ratios, $s_{w,m}$, have been calculated for several
ICRP and ICRU tissues, namely adipose tissue, brain, cortical bone, liver, lung
(deflated and inflated) and spongiosa. The considered clinical beams were 6
and 18 MV x-rays and the field size was 10×10 cm^2. Fluence distributions
were scored at a depth of 10 cm using the Monte Carlo code PENELOPE. The
collision stopping powers for the studied tissues were evaluated employing
the formalism of ICRU Report 37 (1984 Stopping Powers for Electrons and
Positrons (Bethesda, MD: ICRU)). The Bragg–Gray values of $s_{w,m}$ calculated
with these ingredients range from about 0.98 (adipose tissue) to nearly 1.14
(cortical bone), displaying a rather small variation with beam quality. Excellent
agreement, to within 0.1%, is found with stopping-power ratios reported by
Siebers *et al* (2000a *Phys. Med. Biol.* **45** 983–95) for cortical bone, inflated lung
and spongiosa. In the case of cortical bone, $s_{w,m}$ changes approximately 2%
when either ICRP or ICRU compositions are adopted, whereas the stopping-
power ratios of lung, brain and adipose tissue are less sensitive to the selected
composition. The mass density of lung also influences the calculated values of
$s_{w,m}$, reducing them by around 1% (6 MV) and 2% (18 MV) when going from
deflated to inflated lung.

1. Introduction

Quality-assurance procedures for dose-calculation algorithms in radiotherapy treatment-
planning systems involve the comparison of 3D absorbed dose distributions. To this end,

the dose distribution obtained by means of a given algorithm is compared against other Monte Carlo (MC) simulation results or experimental measurements. An important feature, which is not always addressed, is that different clinical calculation methods may yield different quantities related to the absorbed dose for a given tissue. While MC simulations yield the dose to the tissue itself, D_m, traditional correction-based calculation algorithms give the dose to a small water cavity within the tissue, D_w. However, modern convolution/superposition algorithms report D_m as they re-scale the interaction kernels in the traversed media, modelling the energy transfer to the medium. Furthermore, detectors are commonly calibrated in water, and thus measure D_w. A recent comparison of dose distributions and dose-volume indices in clinical plans referring them to D_w versus D_m has revealed large deviations, up to 8%, for head and neck as well as prostate IMRT plans (Dogan *et al* 2006). The question of which quantity should be adopted for comparison purposes is still under debate (Liu and Keall 2002, Dogan *et al* 2006), and there are strong arguments both for using D_m or D_w. Supporters of D_m claim that there is increased uncertainty arising from the introduction of an additional quantity for calculating D_w. On the other hand, those who advocate for the usage of D_w argue that all clinical experience and current dosimetry protocols are D_w based (Almond *et al* 1999, Andreo *et al* 2000). Further reasons that favour the latter position are that the medium employed to report the absorbed dose is always uncertain because the exact composition is not known for real patients (Fippel and Nüsslin 2000, Siebers *et al* 2000b, Liu and Keall 2002, Verhaegen and Devic 2005), and that radiosensitive structures within cells are water-equivalent and may thus be modelled as a water cavity within the medium. What is not under debate is the fact that the dose distributions to be compared must be consistent with each other.

The factor that relates D_m and D_w is $s_{w,m}$, the water/medium stopping-power ratio. Therefore, the importance of the conversion to one of these quantities depends on the value of $s_{w,m}$. Since water is the main component of human tissues, at first sight it would seem that $s_{w,m}$ should not depart too far from unity, so that it is not really a relevant matter. However, for some tissues such as cortical bone, the value of $s_{w,m}$ in clinical photon beams of 6 MV and 18 MV is as high as 1.116 and 1.110, respectively (Siebers *et al* 2000a). As a consequence, misevaluations up to 12% in the absorbed dose could be committed by not taking it into consideration. A similar conclusion has been reached in the case of electron beams, where the observed differences between the dose delivered to a medium and the dose to a water-equivalent medium with the same mass density are 4% for lung and 12% for hard bone (Ding *et al* 2006).

In spite of the interest in this topic, there is only one comprehensive article, published by Siebers *et al* (2000a), in which Bragg–Gray $s_{w,m}$ values for air, lung, soft bone, cortical bone and ICRU tissue were provided for various photon-beam qualities (^{60}Co γ-rays and 4 to 24 MV x-rays). More recently, Jang *et al* (2007) have recalculated stopping-power ratios for the same materials, but along the central axis and using the Spencer–Attix theory, finding generally minor differences with the previous results of Siebers *et al* (2000a).

In the present work, $s_{w,m}$ values for six types of tissue and two x-ray energies (6 and 18 MV) have been obtained by means of the PENELOPE MC code. Some of the considered tissues (inflated lung, spongiosa and cortical bone) match those already studied by Siebers *et al* (2000a), and we include them for comparison purposes. The remaining tissues addressed (adipose tissue, brain, deflated lung and liver) are studied here for the first time. The elemental compositions of the chosen tissues were taken from ICRU Report 44 (ICRU 1989) and ICRP Publication 23 (ICRP 1975) with the aim of quantifying the sensitivity of $s_{w,m}$ to the adopted composition of the medium.

2. Materials and methods

The absorbed dose to (an imaginary small cavity of) water, D_{w}, is related to the absorbed dose to medium, D_{m}, through the simple relation

$$D_{\text{w}} = D_{\text{m}} s_{\text{w,m}}, \tag{1}$$

where $s_{\text{w,m}}$ is the water/medium stopping-power ratio; the subindices w and m refer to water and medium, respectively. In this expression we have omitted additional factors which correct for various perturbation effects in a real detector (Andreo *et al* 2000). In the present study we closely follow the approach of Siebers *et al* (2000a) to compute $s_{\text{w,m}}$. Therefore, in order to circumvent the unnecessary complications of the Spencer–Attix cavity theory[5], we evaluate Bragg–Gray stopping-power ratios instead; these are defined as

$$s_{\text{w,m}} = \frac{\int_0^{E_{\text{max}}} (\Phi_E)_{\text{m}} (S_{\text{col}}/\rho)_{\text{w}}\, \mathrm{d}E}{\int_0^{E_{\text{max}}} (\Phi_E)_{\text{m}} (S_{\text{col}}/\rho)_{\text{m}}\, \mathrm{d}E}, \tag{2}$$

where Φ_E is the fluence, differential in energy, of primary electrons and S_{col}/ρ is the mass collision stopping power. The energy interval covered by the cavity integrals in equation (2) extends from zero to E_{max}, the highest energy encountered in the fluence distribution. However, the tracking of electrons in the MC simulations is limited to energies above the corresponding absorption energy E_{abs}. Siebers *et al* (2000a) split the integrals into two contributions. The larger one, from E_{abs} to E_{max}, is calculated straightforwardly with the MC fluence distributions, whereas the much smaller contribution from zero to E_{abs} is approximated as

$$\int_0^{E_{\text{abs}}} \Phi_E (S_{\text{col}}/\rho)\, \mathrm{d}E \approx \Phi_E(E_{\text{abs}}) \frac{E_{\text{abs}}}{\rho r_{\text{csda}}(E_{\text{abs}})} E_{\text{abs}}, \tag{3}$$

where r_{csda} is the csda range, i.e., a constant fluence distribution $\Phi_E(E_{\text{abs}})$ for $E < E_{\text{abs}}$ and an 'average' mass collision stopping power equal to $E_{\text{abs}}/\rho r_{\text{csda}}(E_{\text{abs}})$ are both assumed.

2.1. MC simulations of Φ_E

2.1.1. Phase-space files. The radiation sources employed in the present simulations were the phase-space files (PSFs) pertaining to the 6 MV ($\text{TPR}_{20,10} = 0.675$) and 18 MV ($\text{TPR}_{20,10} = 0.787$) x-ray beams of the Clinac 1800 (Varian, Palo Alto, USA) linear accelerator previously located at the Hospital de la Santa Creu i Sant Pau, Barcelona. These PSFs were generated using the PENELOPE MC code system (Salvat *et al* 2006) and the PENEASY user code (Sempau 2006); the latter is a structured main program that includes several tallies and source models. The geometry of the accelerator head was modelled following the specifications of the manufacturer (Varian Oncology System), as described elsewhere (Duch *et al* 2006). A $10 \times 10\ \text{cm}^2$ square field (SSD equal to 100 cm) was considered. Particles reaching a plane located 75 cm downstream from the target were recorded in the PSFs. To reduce simulation time, the computation was paralleled on a cluster of 16 CPUs (Pentium IV at 3 GHz) with the CLONEASY package (Badal and Sempau 2006), which enables the simulation to be run on different computers with independent sequences of random numbers.

To validate the PSFs of the beams, additional simulations were carried out in a homogenous water phantom to produce depth-dose curves and lateral profiles. These results were compared with experimental data (Panettieri *et al* 2007) and the values obtained were in reasonably good agreement for the purpose of this work.

---

[5] E.g., the selection of a cut-off energy Δ related to the size of the cavity.
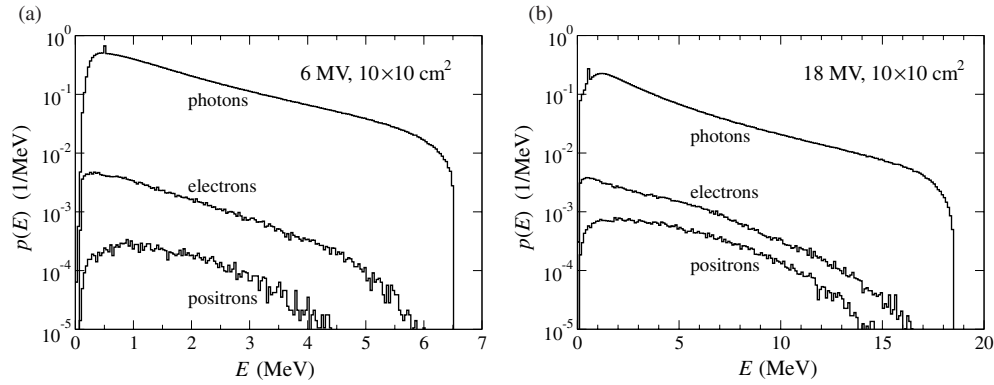
Figure 1. Energy distributions of photons, electrons and positrons in the PSFs of the simulated (a) 6 MV and (b) 18 MV clinical beams. For each type of particle i (= photon, electron or positron) in a given PSF, the integral of its energy distribution is equal to $N_i / \sum_i N_i$, where N_i is the number of particles of that type in the PSF.

The energy distributions of particles stored in the PSFs of the 6 and 18 MV beams are shown in figure 1. Apart from the typical bremsstrahlung energy spectra of megavoltage photon beams, a small contamination of secondary electrons and positrons is present.

2.1.2. Fluence scoring. The aforementioned PSFs were regarded as particle sources for subsequent simulations in homogeneous $50 \times 50 \times 50$ cm^3 phantoms made of adipose tissue, brain, cortical bone, liver, deflated or inflated lung and spongiosa. A splitting factor equal to 4 was applied to the particles in the two PSFs so as to achieve statistical uncertainties lower than 0.1% in the calculated stopping-power ratios. The transport of photons, electrons and positrons was discontinued below $E_{abs} = 7.5$ keV, the same absorption energy as that selected by Siebers *et al* (2000a). The simulation parameters specific of the PENELOPE code (Salvat *et al* 2006) were given conservative values, specifically $C_1 = C_2 = 0.02$, $W_{cc} = 0.1$ keV, $W_{cr} = E_{abs} = 7.5$ keV and $s_{max} = 0.2$ mm.

The fluence was scored 'inside the field' (Siebers *et al* 2000a) in a small volume $V = 4 \times 4 \times 0.1$ cm^3 with its large surfaces perpendicular to the beam and centred on the central axis; the scoring volume was situated at a depth of 10 cm unless otherwise indicated. The user code PENEASY (Sempau 2006) was employed to tally the average fluence distribution in V,

$$\bar{\Phi}_E = \frac{1}{V} \int_V \Phi_E(\vec{r}) \, dV, \tag{4}$$

from the accumulated track-lengths of primary electrons; a logarithmic energy grid with 200 bins (Andreo 1988) was adopted. Due to the smallness of V and the slow variation with depth of the photon fluence distribution in a megavoltage photon beam (Nahum 1978), we can safely assume that the replacement of Φ_E by $\bar{\Phi}_E$ in equation (2) does not affect the calculated stopping-power ratios.

2.2. Mass collision stopping powers

The cavity integrals in equation (2) involve the mass collision stopping powers of water and the various considered media. We follow the formalism described in ICRU Report 37 (ICRU 1984) to calculate S_{col}/ρ. It is based on the Bethe–Bloch formula which, for a given

Table 1. Mean excitation energies of the studied ICRP and ICRU tissues.

Tissue	I (eV)
Adipose tissue (ICRP)	63.2
Adipose tissue (ICRU)	64.8
Brain (ICRP)	73.3
Brain (ICRU)	73.9
Cortical bone (ICRP)	106.4
Cortical bone (ICRU)	112.0
Liver (ICRU)	74.8
Lung (ICRP)[a]	75.3
Lung (ICRU)[a]	75.2
Spongiosa (ICRU)	78.4

[a] Both deflated and inflated.

material, requires its composition, mean excitation energy I and energy-dependent density-effect correction $\delta(E)$ as an input. For liquid water and the ICRP tissues we have taken this information from ICRU Report 37 (ICRU 1984) or the database in the ESTAR program of Berger *et al* (2005). On the other hand, for the ICRU tissues we use the compositions in table 4.4 from (ICRU 1989). The I values were evaluated according to the modified additivity rule for compounds outlined in section 5 of (ICRU 1984), and are listed in table 1 for the sake of completeness. In turn, the $\delta(E)$ functions were obtained by employing the ESTAR program (Berger *et al* 2005). The mass collision stopping powers calculated in this manner are in excellent agreement with values of S_{col}/ρ in table B.1 from (ICRU 1989).

3. Results and discussion

Figure 2 displays Φ_E distributions at a depth of 1.5 cm in water. Our simulation results using PENELOPE are compared with those reported for this particular depth by Siebers *et al* (2000a), who employed the MCNP code. There is good agreement for both the 6 and 18 MV x-rays, in spite of the fact that the actual qualities of the clinical beams simulated by those authors may not be identical to ours.
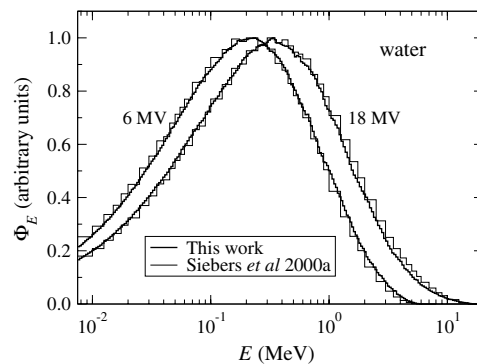

Figure 2. Fluence distributions in water, at a depth of 1.5 cm, corresponding to the 6 and 18 MV beams. The thick and thin histograms are simulation results of the present work and from Siebers *et al* (2000a), respectively.

Table 2. Bragg–Gray (BG) and Spencer–Attix (SA) water/air stopping-power ratios, at a depth of 10 cm, for the indicated photon beams. The tabulated values of $s_{w,a}$ are those calculated in the present study and the ones obtained by Siebers *et al* (2000a) and Jang *et al* (2007).

Beam	This work (BG)	Siebers *et al* (BG)	This work (SA)	Jang *et al* (SA)
6 MV	1.115	1.117	1.119	1.119
18 MV	1.087	1.085	1.091	1.086

Table 3. Water/medium stopping-power ratios of the studied ICRP and ICRU tissues, at a depth of 10 cm, for the 6 MV beam.

Tissue	This work	Siebers *et al*
Adipose tissue (ICRP)	0.978	
Adipose tissue (ICRU)	0.985	
Brain (ICRP)	1.000	
Brain (ICRU)	1.004	
Cortical bone (ICRP)	1.117	1.116
Cortical bone (ICRU)	1.138	
Liver (ICRU)	1.010	
Lung, deflated (ICRU)	1.010	
Lung, inflated (ICRP)	1.000	
Lung, inflated (ICRU)	0.998	0.999
Spongiosa (ICRU)	1.035	1.035

As a further check of our calculation procedure, we have evaluated water/air stopping-power ratios using equation (2) but with $(\Phi_E)_m$ replaced by $(\Phi_E)_w$ in the integrals. The calculated $s_{w,a}$ ratios, at a depth of 10 cm in water, are listed in table 2 and compared with the values given by Siebers *et al* (2000a). There is very good accordance between both sets, with differences of a mere 0.2%, confirming the consistency of our methodology with theirs. As a final verification, Spencer–Attix water/air stopping-power ratios (see, e.g., Andreo (1988)) have also been calculated[6] for the 6 and 18 MV beams; the corresponding values are included in table 2. The discrepancy between the Bragg–Gray and Spencer–Attix results is only 0.4%, indicating that the Bragg–Gray formalism is suitable when the sought for accuracy in the application under consideration is of the order of 0.5%. In fact one could even neglect the contribution of the track-ends, equation (3), because this would modify the stopping-power ratios presented below by at most 0.2%. Nevertheless we prefer to keep this term because it is estimated in a very simple way and, moreover, a strict comparison of our results with those of Siebers *et al* (2000a), who did include it, is then possible.

The main results of our work, i.e. the Bragg–Gray $s_{w,m}$ ratios for the selected tissues and beams, are presented in tables 3 and 4. Remarkable agreement is found with the data by Siebers *et al* (2000a) for ICRP cortical bone, ICRU inflated lung and ICRU spongiosa; the largest discrepancy is 0.1%. Jang *et al* (2007) have recently calculated Spencer–Attix stopping-power ratios for these three materials. The present values are compatible with theirs, confirming that the choice of cavity theory has a limited impact on the calculated results (Jang *et al* 2007). The values of $s_{w,m}$ for the other tissues studied here range from approximately 0.98 (adipose tissue) to nearly 1.14 (cortical bone). In most cases, variation with photon

---

[6] Setting $\Delta = 10$ keV, the conventional cut-off energy used in the dosimetry with ion chambers.

Table 4. Water/medium stopping-power ratios of the studied ICRP and ICRU tissues, at a depth of 10 cm, for the 18 MV beam. The values by Siebers *et al* (2000a) are obtained by linear interpolation from their results for 15 and 24 MV beams.

Tissue	This work	Siebers *et al*
Adipose tissue (ICRP)	0.981	
Adipose tissue (ICRU)	0.988	
Brain (ICRP)	1.001	
Brain (ICRU)	1.005	
Cortical bone (ICRP)	1.111	1.110
Cortical bone (ICRU)	1.131	
Liver (ICRU)	1.011	
Lung, deflated (ICRU)	1.010	
Lung, inflated (ICRP)	0.988	
Lung, inflated (ICRU)	0.987	0.986
Spongiosa (ICRU)	1.035	1.035

beam quality is rather small, less than 0.3%, except for cortical bone, where it reaches 0.7%. Furthermore, $s_{w,m}$ is almost constant as a function of depth (results not shown).

When, for a given tissue, ICRP Publication 23 (ICRP 1975) and ICRU Report 44 (ICRU 1989) recommend elemental compositions which are not identical, the corresponding $s_{w,m}$ values can also differ. The stopping-power ratios of inflated lung calculated using the compositions from either ICRP or ICRU are similar, within 0.1–0.2%. Brain and adipose tissue display a moderate change with composition, 0.4% and 0.7%, respectively, regardless of the beam quality. The variation is much larger for cortical bone, approximately 2%. The case of ICRU lung requires a further comment. The change in the $s_{w,m}$ value between deflated and inflated lung is very large too, 1.2% and 2.3% for the 6 and 18 MV qualities, respectively, thus increasing with the $TPR_{20,10}$ of the beam. This behaviour has its origin in the density-effect correction, which increases with the mass density of the medium and the electron energy. As a consequence, the mass collision stopping power of deflated lung is lower than that of the inflated organ, especially for the 18 MV beam, leading to the observed trends of the calculated $s_{w,m}$ data for this tissue.

4. Conclusions

We have calculated water/medium stopping-power ratios for various ICRP and ICRU tissues. To this end, we have simulated fluence distributions with the MC code PENELOPE for 6 and 18 MV beams, and used mass collision stopping powers evaluated by means of the formalism described in ICRU Report 37.

The value of $s_{w,m}$ is close to 1 for most soft tissues and both beam energies. On the other hand, the departure of $s_{w,m}$ from unity is 3.5% for spongiosa and up to almost 14% for cortical bone. Large differences in absorbed dose distributions depending on whether the reported quantity is D_w or D_m can then be expected for such bone-like tissues.

The rather extreme case of cortical bone deserves, however, a word of caution. It could turn out that the present stopping-power ratios of this material are not identical to the ratios of absorbed doses due to the perturbation factors disregarded in equation (1) not being equal to 1 for a cavity of finite volume. Exploratory simulations we have performed indicate that for cortical bone D_w/D_m would be somewhat lower than the values of $s_{w,m}$ displayed in tables 3 and 4. Unfortunately the direct calculation of D_w/D_m is much more inefficient

than the evaluation of $s_{w,m}$ from fluence distributions. The ensuing simulations are thus time-consuming, particularly if one defines smaller scoring volumes in order to reduce the perturbation caused to Φ_E by the material in the cavity. Such problems prevent us from reaching definite conclusions at this stage.

The choice of a particular elemental composition for a certain tissue may significantly affect the value of $s_{w,m}$ depending on the type of tissue and, to a lesser extent, the beam quality. For cortical bone, the variation of $s_{w,m}$ with composition is around 2%. These differences come from the mean excitation energy, which is a function of the elemental composition, that determines the mass collision stopping power. Besides, the specific mass density adopted for lung also affects the corresponding stopping-power ratios, a direct result of the growing importance of the density-effect correction to S_{col}/ρ as the beam energy increases. The observed changes in $s_{w,m}$ are 1.2% and 2.3% for the 6 and 18 MV clinical x-ray beams, respectively. As a consequence of these findings, the main source of uncertainty in the transformation of dose to medium into dose to water is the exact composition (and mass density) of each voxel (Verhaegen and Devic 2005).

For the studied tissues, the value of $s_{w,m}$ depends weakly on the depth and the quality of the megavoltage photon beam. Therefore, for clinical purposes, the use of a single value assigned to each tissue would not increase the uncertainty dramatically, once all sources of uncertainty are taken into consideration; this is a pragmatic approach adopted by several authors; see, e.g., Carrasco *et al* (2004), Paelinck *et al* (2005) and Sterpin *et al* (2007). However, comparison of absorbed doses at the 1% level would require a precise knowledge of the composition of the involved tissues, which is not affordable in clinical situations.

Acknowledgments

References

Almond P R, Biggs P J, Coursey B M, Hanson W F, Huq M S, Nath R and Rogers D W O 1999 AAPMs TG-51 protocol for clinical reference dosimetry of high-energy photon and electron beams *Med. Phys.* **26** 1847–70

Andreo P 1988 Stopping-power ratios for dosimetry *Monte Carlo Transport of Electrons and Photons* ed T M Jenkins, W R Nelson and A Rindi (New York: Plenum) pp 485–501

Andreo P, Burns D T, Hohlfeld K, Huq M S, Kanai T, Laitano F, Smyth V and Vynckier S 2000 Absorbed Dose Determination in External Beam Radiotherapy: An International Code of Practice for Dosimetry Based on Standards of Absorbed Dose to Water *IAEA Technical Reports Series no 398* (Vienna: International Atomic Energy Agency)

Badal A and Sempau J 2006 A package of Linux scripts for the parallelization of Monte Carlo simulations *Comput. Phys. Commun.* **175** 440–50

Berger M J, Coursey J S and Zucker M A 2005 programs ESTAR, PSTAR and ASTAR, http://physics.nist.gov/PhysRefData/Star/Text/contents.html

Carrasco P, Jornet N, Duch M A, Weber L, Ginjaume M, Eudaldo T, Jurado D, Ruiz A and Ribas M 2004 Comparison of dose calculation algorithms in phantoms with lung equivalent heterogeneities under conditions of lateral electronic disequilibrium *Med. Phys.* **31** 2899–911

Ding G X, Duggan D M, Coffey C W, Shokrani P and Cygler J E 2006 First macro Monte Carlo based commercial dose calculation module for electron beam treatment planning—new issues for clinical consideration *Phys. Med. Biol.* **51** 2781–99

Dogan N, Siebers J V and Keall P J 2006 Clinical comparison of head and neck and prostate IMRT plans using absorbed dose to medium and absorbed dose to water *Phys. Med. Biol.* **51** 4967–80

Duch M A, Carrasco P, Ginjaume M, Jornet N, Ortega X and Ribas M 2006 Dose evaluation in lung-equivalent media in high-energy photon external radiotherapy *Radiat. Prot. Dosim.* **120** 43–7

Fippel M and Nüsslin F 2000 Comments on 'Converting absorbed dose to medium to absorbed dose to water for Monte Carlo based photon beam dose calculations' *Phys. Med. Biol.* **45** L17–8

ICRP (International Commission on Radiological Protection) 1975 Report of the Task Group on Reference Man *ICRP Publication No. 23* (Oxford: Pergamon)

ICRU (International Commission on Radiation Units and Measurements) 1984 Stopping Powers for Electrons and Positrons *ICRU Report 37* (Bethesda, MD: ICRU)

ICRU (International Commission on Radiation Units and Measurements) 1989 Tissue Substitutes in Radiation Dosimetry and Measurement *ICRU Report 44* (Bethesda, MD: ICRU)

Jang S Y, Liu H H, Mohan R and Siebers J V 2007 Variations in energy spectra and water-to-material stopping-power ratios in three-dimensional conformal and intensity-modulated photon fields *Med. Phys.* **34** 1388–97

Liu H H and Keall P 2002 D_m rather than D_w should be used in Monte Carlo treatment planning *Med. Phys.* **29** 922–4

Nahum A E 1978 Water/air mass stopping power ratios for megavoltage photon and electron beams *Phys. Med. Biol.* **23** 24–38

Paelinck L, Reynaert N, Thierens H, De Neve W and De Wagter C 2005 Experimental verification of lung dose with radiochromic film: comparison with Monte Carlo simulations and commercially available treatment planning systems *Phys. Med. Biol.* **50** 2055–69

Panettieri V, Duch M A, Jornet N, Ginjaume M, Carrasco P, Badal A, Ortega X and Ribas M 2007 Monte Carlo simulation of MOSFET detectors for high-energy photon beams using the PENELOPE code *Phys. Med. Biol.* **52** 303–16

Salvat F, Fernández-Varea J M and Sempau J 2006 *PENELOPE-2006: A Code System for Monte Carlo Simulation of Electron and Photon Transport* (Issy-les-Moulineaux: NEA/OECD)

Sempau J 2006 PENEASY, a structured main program for PENELOPE, freely available from http://www.upc.es/inte/downloads/penEasy.htm

Siebers J V, Keall P J, Nahum A E and Mohan R 2000a Converting absorbed dose to medium to absorbed dose to water for Monte Carlo based photon beam dose calculations *Phys. Med. Biol.* **45** 983–95

Siebers J V, Keall P J, Nahum A E and Mohan R 2000b Reply to 'Comments on 'Converting absorbed dose to medium to absorbed dose to water for Monte Carlo based photon beam dose calculations' *Phys. Med. Biol.* **45** L18–9

Sterpin E, Tomsej M, De Smedt B, Reynaert N and Vynckier S 2007 Monte Carlo evaluation of the AAA treatment planning algorithm in a heterogeneous multilayer phantom and IMRT clinical treatments for an Elekta SL25 linear accelerator *Med. Phys.* **34** 1665–77

Verhaegen F and Devic S 2005 Sensitivity study for CT image use in Monte Carlo treatment planning *Phys. Med. Biol.* **50** 937–46